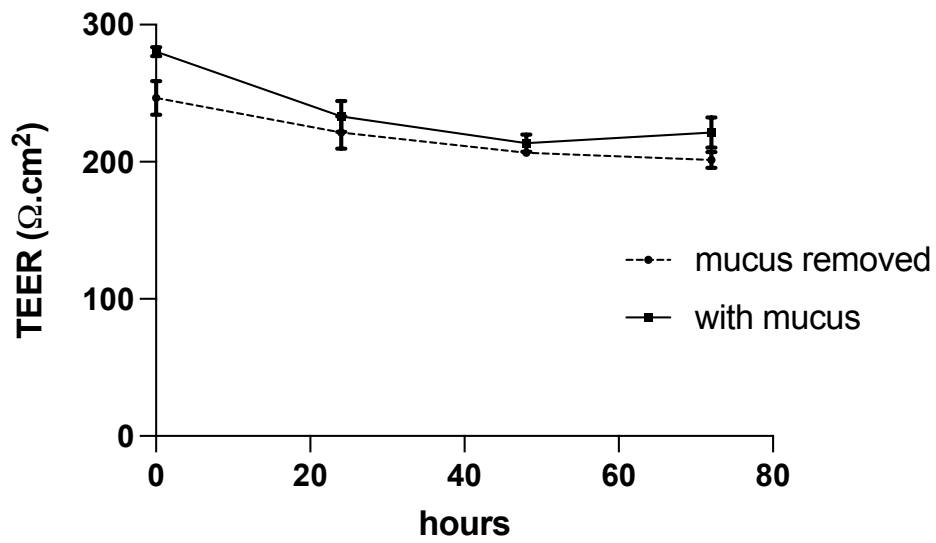
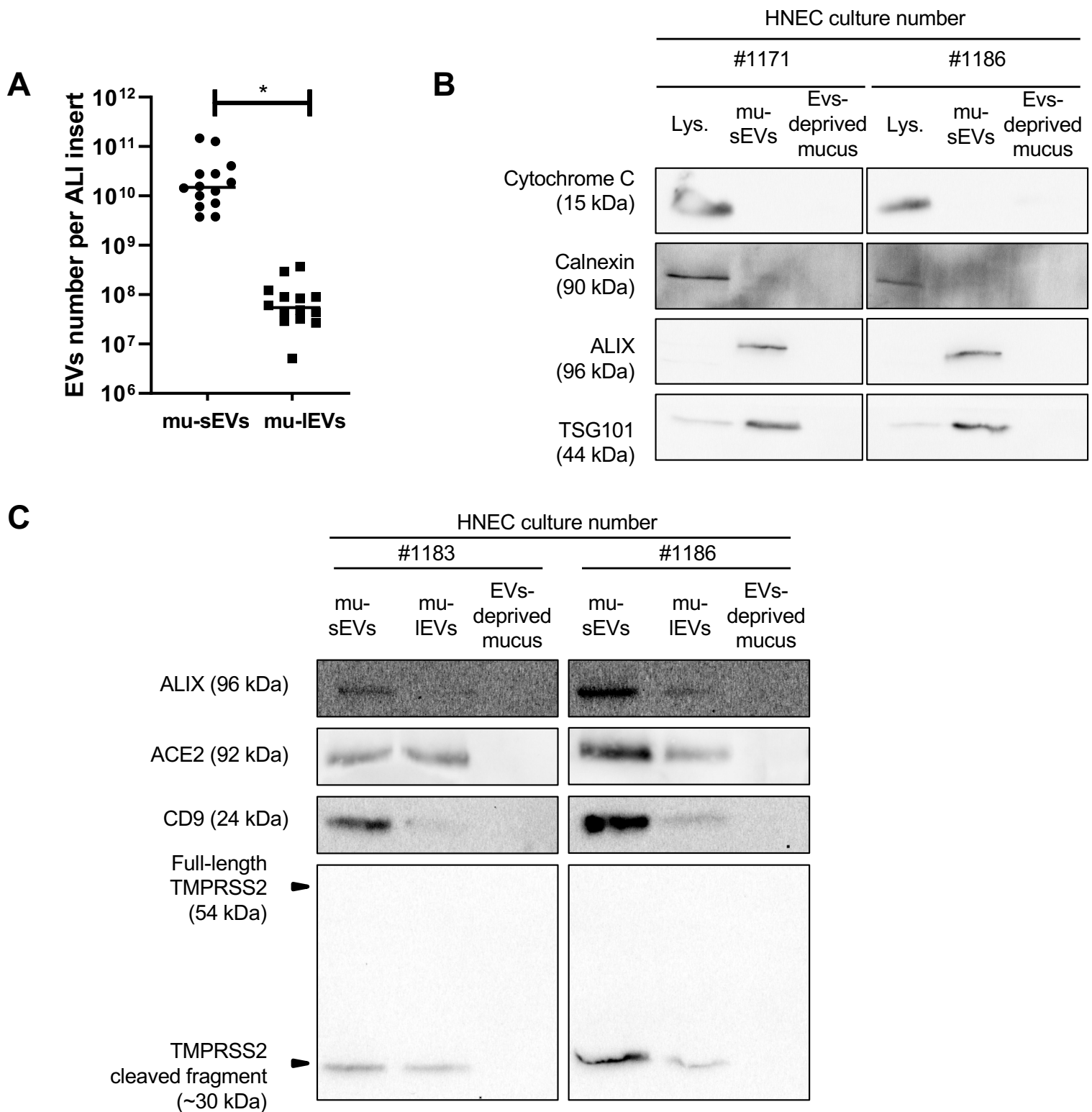


## Supplementary Figure 1



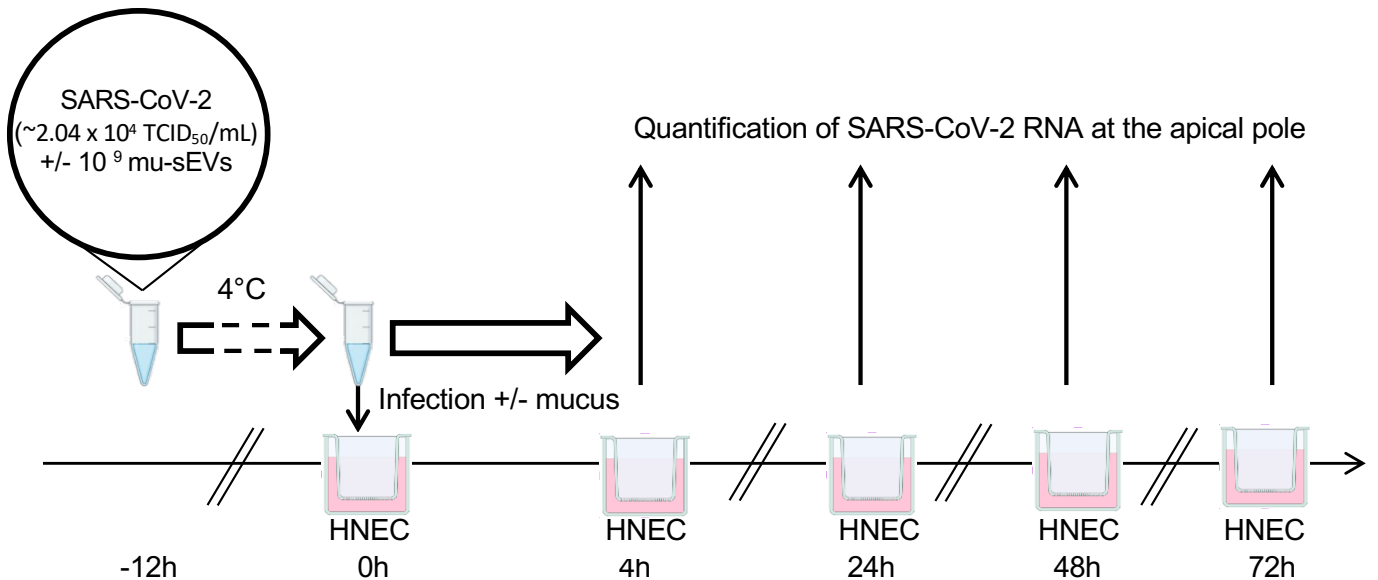
**Supplementary Figure 1 legend. Effect of mucus removal on HNECs vitality.** HNECs vitality as reflected by the trans-epithelial electrical resistance (TEER) measured in untreated or mucus-removed samples from two distinct patients, at different time-points.

## Supplementary Figure 2



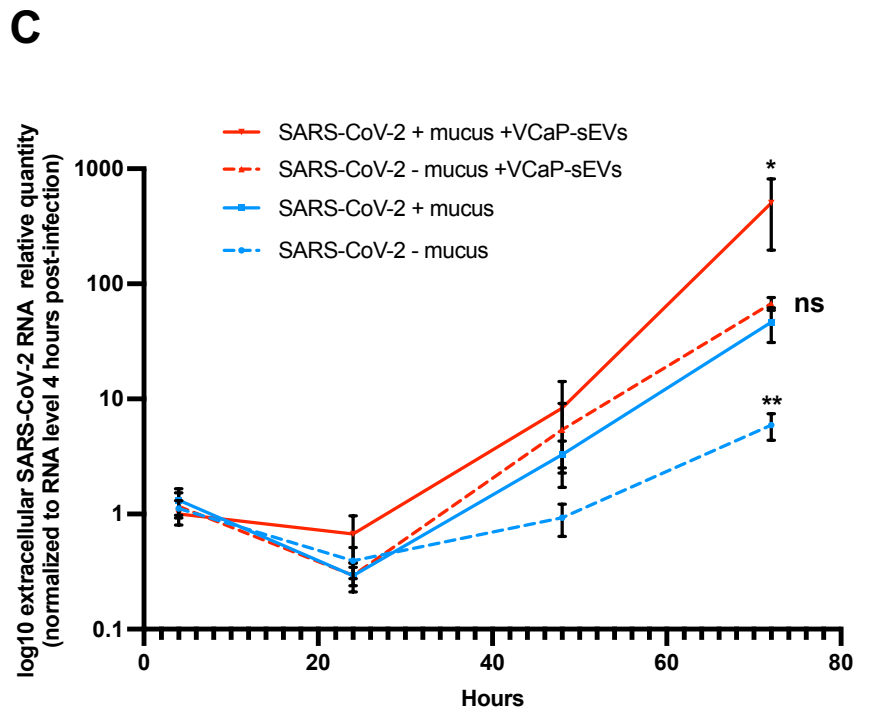
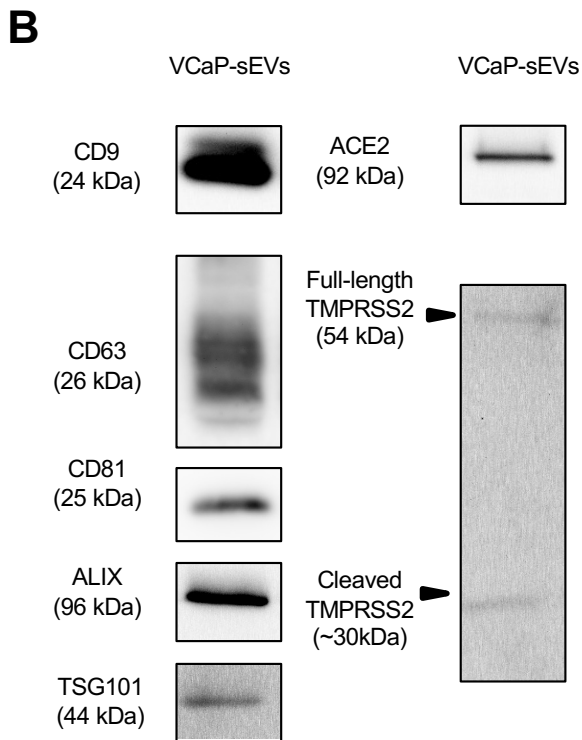
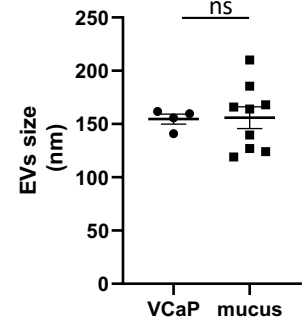
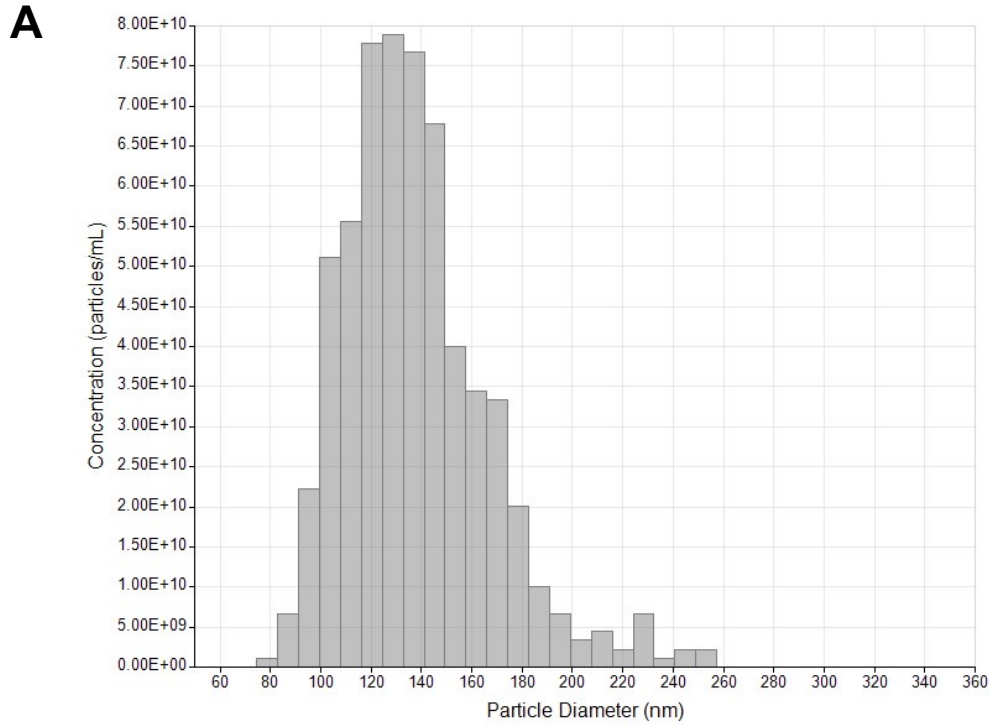
**Supplementary Figure 2 legend. Characterization of EVs isolated from HNECs from distinct patients. (A)** EVs produced by HNECs from 14 different patients analyzed by tunable resistive pulse sensing (TRPS) showing mean particles concentrations of  $3.3 \pm 1.2 \times 10^{10}$  mu-sEVs (small extracellular vesicles) and  $9.6 \pm 2.8 \times 10^7$  mu-IEVs (large extracellular vesicles) per ALI insert. **(B)** Western blot analysis of cytochrome C, Calnexin, ALIX and TSG101 using 10  $\mu$ g of protein of HNECs lysates, mu-sEVs and EVs-deprived mucus. **(C)** Western blot analysis of CD9, ALIX, ACE2 and full-length and cleaved TMPRSS2 using 5  $\mu$ g of protein of mu-sEVs, mu-IEVs and EVs-deprived mucus. \* $p < 0.05$ .

### Supplementary Figure 3



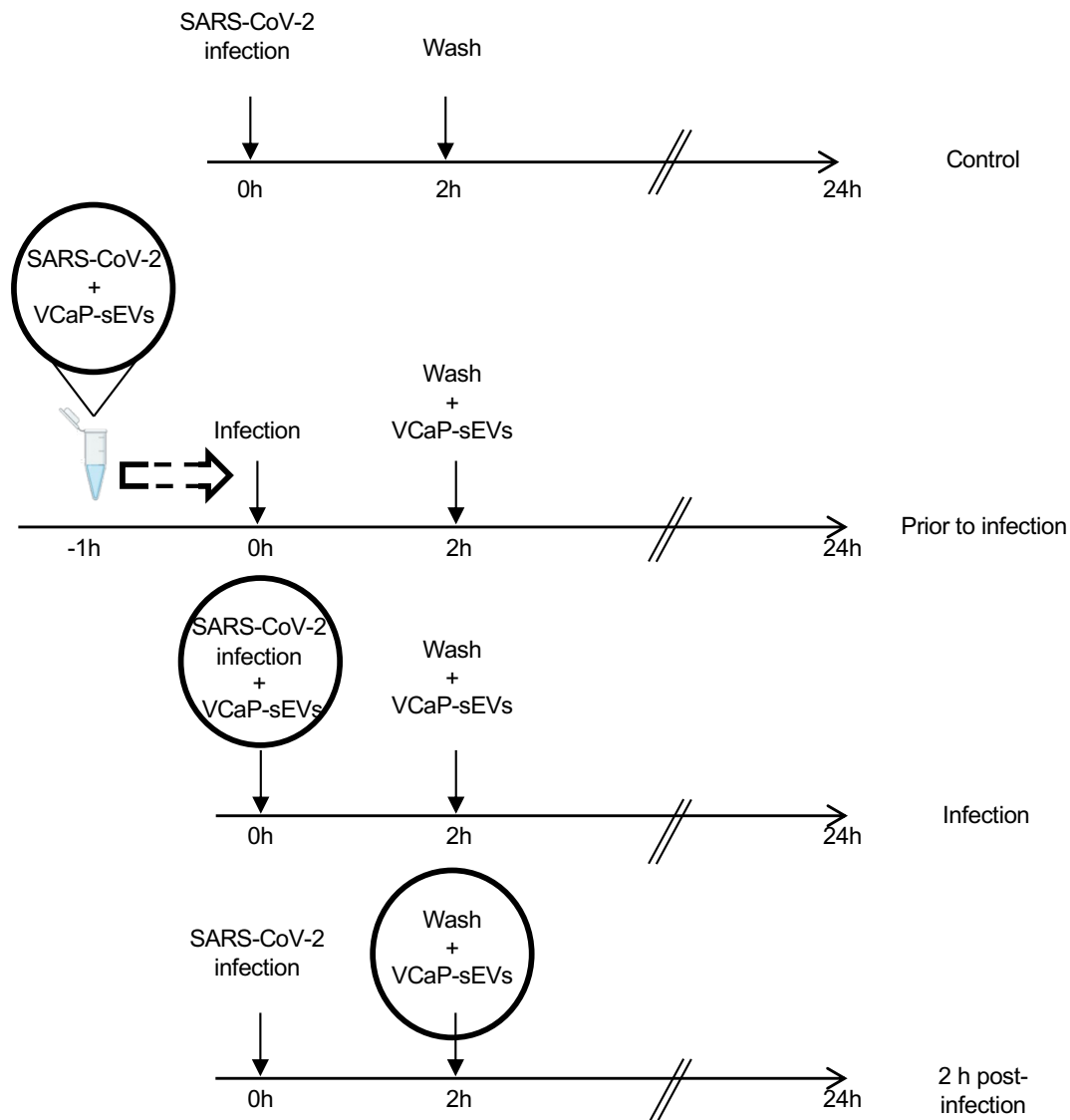
**Supplementary Figure 3 legend. Effect of mu-sEVs and mucus-containing sEVs on HNEC infection by SARS-CoV-2: Experimental design.** SARS-CoV-2 particles (10  $\mu$ L of viral inoculum,  $\sim 2.04 \times 10^5$  TCID<sub>50</sub>/mL) were incubated overnight at 4°C with  $10^9$  mu-sEVs from two different patients or with PBS in 100  $\mu$ L final volume. Infection (20  $\mu$ L of the mixture) was performed at the apical pole of HNECs isolated from a third, different, patient, in the presence or after removal of recipient cell mucus. Viral RNA was recovered at the apical pole at different time points post-infection and quantified.

# Supplementary Figure 4



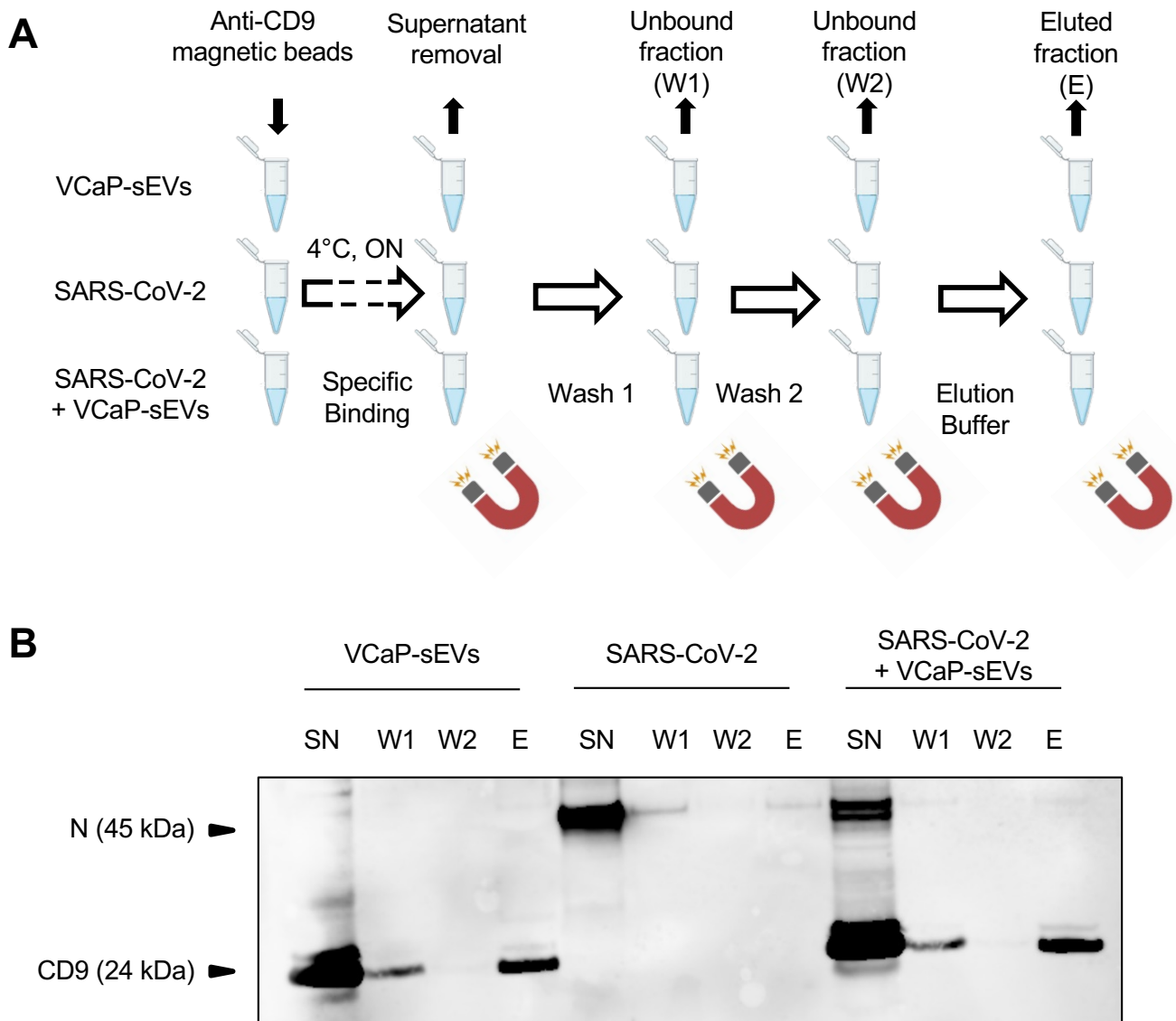
**Supplementary Figure 4 legend. Characterization of VCaP-sEVs and effect on HNEC infection by SARS-CoV-2. (A)** sEVs isolated from 4 independent VCaP cell cultures analyzed by tunable resistive pulse sensing (TRPS) showing a mean peak VCaP-sEV size of approximately ~150 nm in diameter. Left panel: histogram generated from one representative VCaP culture. Right panel: comparison of VCaP-sEV vs mu-sEV (mucus) sizes. **(B)** Western blot analysis of VCaP-sEV markers (CD9, CD63, CD81, ALIX, TSG101) and SARS-CoV-2 entry factors (ACE2 and TMPRSS2). **(C)** Dynamics of SARS-CoV-2 RNA production at the apical pole of HNECs isolated from two patients assessed by RT-qPCR. SARS-CoV-2 viral particles were preincubated with  $10^9$  VCaPs or PBS, overnight at 4°C, and HNECs infection in absence or presence of recipient cell mucus was performed as described in figure 2A. Results were normalized to the time-point 4 hours for each condition and expressed as log<sub>10</sub> mean ± SEM of two independent experiments. \* $p$  <0.05, \*\* $p$  <0.01 (Mann-whitney U-test).

## Supplementary Figure 5



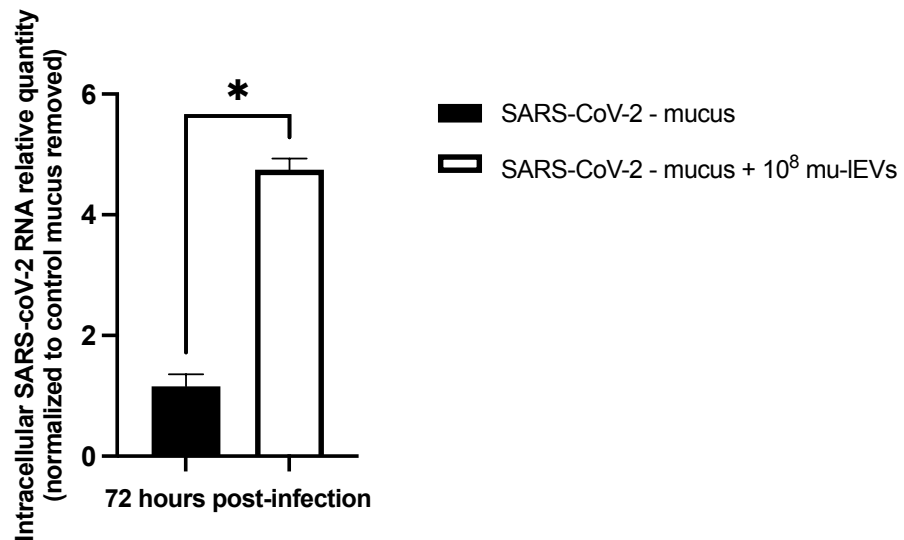
**Supplementary Figure 5 legend. Design of time-of-addition experiments.** Calu-3 cells were infected with SARS-CoV-2 virus not incubated with VCaP-sEVs (control) or incubated with VCaP-sEVs for 1 hour prior to infection, added at the time of infection or added 2 hours post-infection. Cells were washed 2 hours post-infection, and culture medium containing VCaP-sEVs was added. Infections were performed at a final MOI of 1 and  $10^9$  VCaP-sEVs were used. Intracellular RNA was extracted 24 hours post-infection and quantified by means of RT-qPCR.

## Supplementary Figure 6



**Supplementary Figure 6 legend. SARS-CoV-2/VCaP-sEV fusion assay. (A)** Experimental Design. Exosome-human CD9 isolation beads (100  $\mu$ L) were incubated with  $10^{10}$  VCaP-sEVs, SARS-CoV-2 viral particles (10  $\mu$ L viral inoculum,  $\sim 2.04 \times 10^4$  TCID<sub>50</sub>) or a mixture of both in PBS -/- (final volume 100 mL) at 4°C overnight (ON) on a rotating wheel. All samples were placed on a magnetic separator and supernatants (SN) were collected. Two washings (300  $\mu$ L PBS) were performed sequentially and collected using a magnetic separator (W1, W2). Finally, beads were resuspended in 50  $\mu$ L EZ buffer (E) before denaturation at 95°C and analysis by western blot. **(B)** Western blot analysis of CD9 and N proteins in all fractions collected in (A).

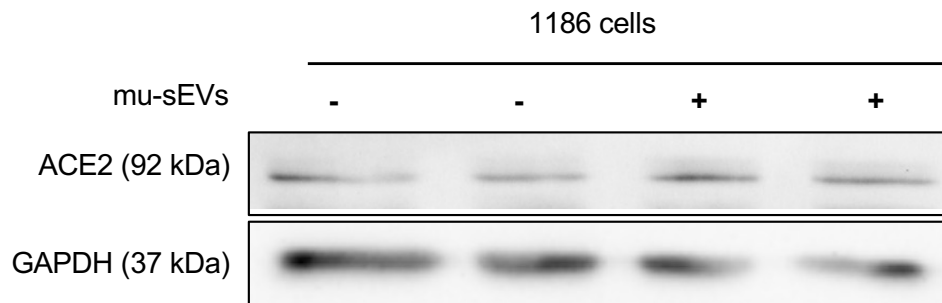
## Supplementary Figure 7



**Supplementary Figure 7 legend. Effect of mu-IEVs on HNECs infection by SARS-CoV-2.** Preincubations were performed under gentle agitation, overnight at 4°C, using SARS-CoV-2 viral particles (10  $\mu$ L of viral inoculum,  $\sim 2.04 \times 10^5$  TCID<sub>50</sub>/mL) and PBS or  $10^8$  mu-IEVs in 100  $\mu$ L final volume. Infection was performed at the apical pole of HNECs, after removal of cell produced-mucus. Intracellular SARS-CoV-2 RNA was extracted 72 hours post-infection and was quantified by RT-qPCR. Results were normalized to 18S rRNA, then to control without mucus and viral particles preincubation with PBS (black bar). They are expressed as mean $\pm$ SEM of two independent experiments. \*  $p < 0.05$ .



## Supplementary Figure 8



**Supplementary Figure 8 legend. Effect of mu-sEVs incubation on ACE2 expression in HNECs cells.** Western blot analysis of ACE2 and GAPDH proteins in HNECs lysates, after incubation of HNECs with  $10^9$  mu-sEVs or PBS for 4 hours.